J. Fluid Mech. (2002), *vol.* 466, *pp.* 305–318. © 2002 Cambridge University Press
DOI: 10.1017/S0022112002001246 Printed in the United Kingdom

On steep gravity waves meeting a vertical wall: a triple instability

By MICHAEL S. LONGUET-HIGGINS[1] AND DAVID A. DRAZEN[2]

[1]Institute for Nonlinear Science, University of California, San Diego, La Jolla, CA 92093-0402, USA

[2] Scripps Institution of Oceanography, University of California, San Diego, La Jolla, CA 92093-0213, USA

(Received 21 October 2001 and in revised form 20 March 2002)

Theoretical arguments suggest that progressive gravity waves incident on a vertical wall can produce periodic standing waves only if the incident wave steepness ak is quite small, certainly less than 0.284. Laboratory experiments are carried out in which an incident wave train of almost uniform amplitude meets a vertical barrier. At wave steepnesses greater than 0.236 the resulting motion near the barrier is non-periodic. A growing instability is observed in which every third wave crest is steeper than its neighbours. The steep waves develop sharp crests, or vertical jets. The two neighbouring crests are rounded, flat-topped, or of intermediate form. The instability grows by a factor of about 2.2 for every three wave periods, almost independently of the incident wave steepness.

1. Introduction

Surface gravity waves of low amplitude, when reflected from a vertical wall, will produce standing waves of double the amplitude of the incident waves. If on the other hand the incident waves are steep enough, they are found to throw up vertical jets of water against the reflecting barrier; see for example Chan & Melville (1988). The same phenomenon is often observed when incoming waves meet a cliff or harbour wall. Moreover, this is not merely a shallow-water phenomenon but occurs also in deep water. As will be seen below, it follows from a simple energy argument that progressive waves of more than a certain steepness *cannot* produce periodic standing waves; they must be aperiodic.

In his well-known experiments on steep standing waves Sir Geoffrey Tayor (1954) considered only periodic waves, whose maximum slope he found to be about 45°. In accurate computations Mercer & Roberts (1992) showed that periodic standing waves of given wavelength cannot have more than a certain energy, although at energies slightly below that maximum two different periodic waves having the same energy can exist. Jiang, Perlin & Schultz (1998) have carried out experiments on deep-water standing waves forced subharmonically by a vertical oscillation of the wave tank. It was shown that the waves could be made to break periodically once every three wave 'periods'. Numerical studies of 'super-energetic' standing waves, with various initial conditions, have been carried out by Longuet-Higgins & Dommermuth (2001*a*, *b*) and it was found that either single jets could be produced, which fell back vertically into the trough of the wave, creating a semi-circular cavity, or in other cases, starting

https://doi.org/10.1017/S0022112002001246 Published online by Cambridge University Press

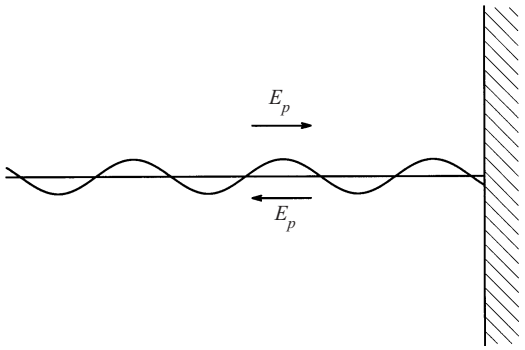


FIGURE 1. Reflection of a progressive wave from a vertical wall, when the maximum surface slope is small.

with a circular cavity, the wave crests could become flat-topped and then break on either side of the wave crest, like a pair of spilling or plunging breakers.

The purpose of the present paper is to describe experiments in which free progressive waves are allowed to impinge on a vertical wall, and the complete history of the motion is then followed. There is no forcing of the wave motion by a vertical or other kind of oscillation of the boundary, apart from the remote wavemaker. It is found that when the steepness ak of the incident wave train exceeds about 0.236 the waves in the neighbourhood of the boundary develop a growing instability in which every third wave (in time) is the steepest, the two intermediate waves having flat-topped or rounded crests, or of a mixed type. The steepest waves become sharp-crested; see § 5. A discussion and conclusions follow in § 6.

2. Energy and periodicity

Some general conclusions may be drawn immediately from a consideration of the total energy density of the waves; see figure 1.

Let E_p denote the mean energy density of the incident progressive wave, averaged over time and horizontal distance. According to the *linearized* theory of surface waves, in which the surface slopes are small, we have

$$E_p = \tfrac{1}{2}\rho g a^2, \tag{2.1}$$

where ρ is the density, g the acceleration due to gravity and a the wave amplitude. The reflected wave is similar, and the two waves combine to form a standing wave of maximum amplitude $2a$ (crest-to-trough height $4a$) and of time-averaged energy

$$E_s = 2E_p. \tag{2.2}$$

Hence

$$E_p = \tfrac{1}{2}E_s. \tag{2.3}$$

According to the linearized theory there is no limit to either E_p or E_s, assuming the wavelength L to be fixed. However from the fully *nonlinear* theory of gravity waves the total energy E_s of a standing wave has a maximum given by

$$(E_s)_{\max} = 0.07774 \tag{2.4}$$

in units where ρ, g and the wavenumber k are all unity; see Mercer & Roberts (1992). Hence, if we assume that all the energy of the incident and the reflected wave goes

https://doi.org/10.1017/S0022112002001246 Published online by Cambridge University Press

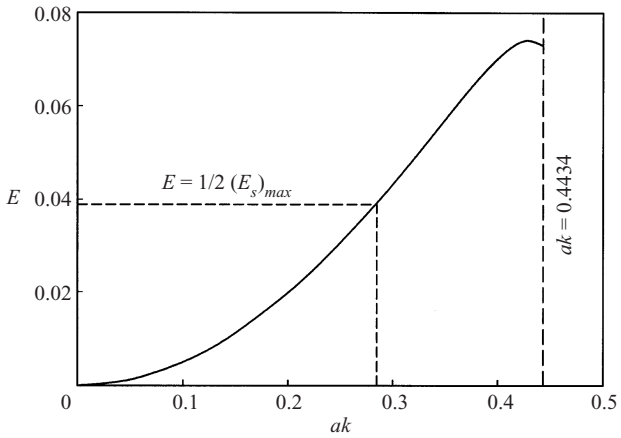


FIGURE 2. Graph of the energy density E_p of a progressive gravity wave of finite steepness ak.

to form a periodic standing wave, and if we ignore the contribution of the higher harmonics to the total energy (but not to the surface profile), then we must have

$$E_p \leqslant \tfrac{1}{2}(E_s)_{\max} = E_{crit} \tag{2.5}$$

say, where from (2.4)

$$E_{crit} = 0.03887. \tag{2.6}$$

If on the other hand $E_p > E_{crit}$ we see that the resulting motion cannot be periodic.

Now a plot of the energy density E_p of a progressive wave against its steepness ak (figure 2) shows that a progressive wave may have an energy as great as

$$(E_p)_{\max} = 0.0745 \tag{2.7}$$

which is achieved when

$$ak = 0.429. \tag{2.8}$$

The maximum wave steepness ak for a progressive wave is 0.4432. So from figure 2 and equation (2.6) there is a certain range of progressive wave steepnesses, namely

$$0.285 < ak < 0.443 \tag{2.9}$$

for an incident wave, such that the incident-plus-reflected wave system cannot be a perfectly periodic standing wave. The resulting motion must be irregular or chaotic in some way, leading possibly to breaking.

Incident progressive waves whose steepness lies in the range $0 < ak < 0.285$ we shall call *subcritical*, while those that lie in the range (2.8) we shall call *supercritical*. It is not of course implied that all subcritical incident waves will necessarily produce motions that are perfectly periodic. This is a matter for experiment.

3. Experimental apparatus

The experiments were carried out in a glass-sided wave tank in the Hydraulics Laboratory at the Scripps Institution of Oceanography. Its dimensions are shown in figure 3. A computer-controlled, horizontal-movement wavemaker was at A, and an impervious, sloping beach with gradient 1 : 10 was at C. A removeable plane wall, or barrier, was inserted at B. The distances AB and AC were 15.65 m and 26.96 m

https://doi.org/10.1017/S0022112002001246 Published online by Cambridge University Press

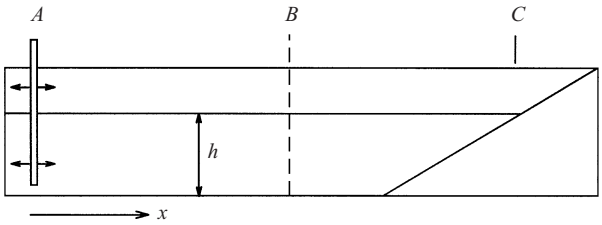


FIGURE 3. Sketch of the wave tank.

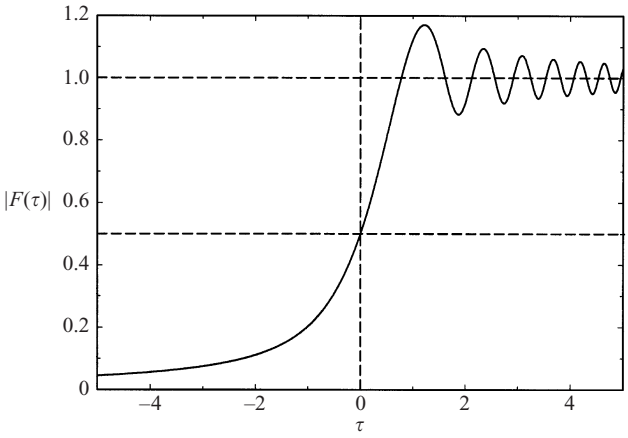


FIGURE 4. Theoretical envelope of the surface elevation in the neighbourhood of a wave front, from equation (4.1).

respectively. The width W of the tank and the stillwater depth h were both equal to 0.50 m.

The vertical displacement of the water surface was measured with resistence-wire gauges, each consisting of two parallel vertical wires separated by 0.3 cm and oriented across the tank at B, near the mid-plane of the wave tank. With the barrier in place, the wires were 2 mm from the surface of the wall. Calibration before and after each run indicated that the gauges were linear to within about 1% over the range of measurement. The output from the gauges was digitized and recorded at a rate of 100 Hz.

A video recording of the surface at a rate of 30 frames/s was made from a position slightly above the mean water level and to the left (wave side) of the barrier. Blue vegetable dye was added to the water to increase the contrast between air and water, the background on the far wall being white.

4. Procedure

The experiments were conducted at a wave frequency $f = 1.0$ or $1.1\,\mathrm{s}^{-1}$, which is somewhat less than the cut-off frequency ($1.25\,\mathrm{s}^{-1}$) for the lowest-order three-dimensional waves in a channel of width 0.5 m. Nevertheless, after a certain duration (about 45 s) some higher-order three-dimensional instabilities invariably made their appearance. The most prominent of these was a cross-wave with wavelength 25 cm (half the width of the channel) which appeared when $f = 1.0\,\mathrm{s}^{-1}$. Therefore most experiments were done at $f = 1.1\,\mathrm{s}^{-1}$.

https://doi.org/10.1017/S0022112002001246 Published online by Cambridge University Press

G	a_o (cm)	a (cm)	$a\sigma^2/g$	ak	a_s (cm)
1.6	4.53	4.22	0.206	0.200	7.50
1.8	5.19	4.63	0.226	0.216	6.95
2.0	5.52	5.66	0.251	0.236	7.87
2.2	5.82	5.51	0.268	0.252	8.49
2.4	6.61	5.85	0.285	0.266	9.28
2.6	7.52	6.36	0.310	0.285	10.89

TABLE 1. Range of experiments with $\lambda = 0.1$, $N = 40$; ak is determined by the procedure described in the Appendix.

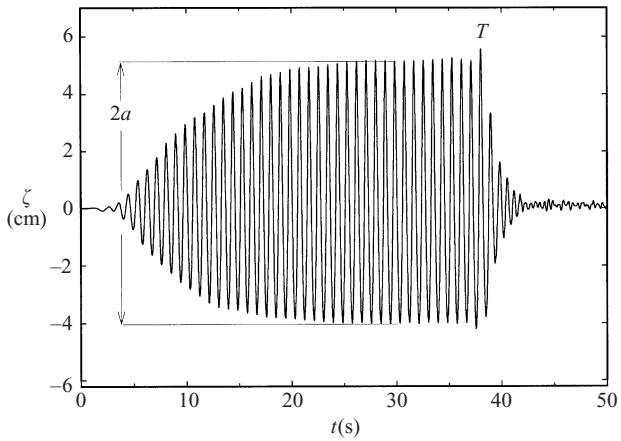


FIGURE 5. Record of the surface elevation at $x = 2.30\,\mathrm{m}$ when $\lambda = 0.1$ and $N = 40$ (progressive wave: $G = 1.6$).

As is well known, if a wavemaker is started from rest, the wave front advances down the channel with the group velocity c_g. If the wavemaker is switched on suddenly at time $t = 0$, then according to linear theory the surface elevation $\zeta(x,t)$ at a horizontal distance x from the wavemaker is given by

$$\zeta = \mathrm{i}BF(\tau)\mathrm{e}^{\mathrm{i}\sigma(t-\sigma x/g)} \tag{4.1}$$

approximately, where B is a constant depending on the type of wavemaker, σ is the radian frequency of the waves, τ is a dimensionless time:

$$\tau = \left(\frac{g}{2\pi x}\right)^{1/2}\left(t - \frac{2\sigma x}{g}\right) \tag{4.2}$$

which vanishes at the wave front $t = 2\sigma x/g$, and $F(\tau)$ describes the complex wave envelope:

$$F(\tau) = \frac{1}{2} + \frac{1}{1+\mathrm{i}}\int_0^\tau \mathrm{e}^{\mathrm{i}\pi\mu^2/2}\,\mathrm{d}\mu; \tag{4.3}$$

see for example Miles (1962). The function $F(\tau)$ is related to the Fresnel integral (Abramowitz & Stegun 1964). A sketch of the envelope $|F(\tau)|$ as a function of time is shown in figure 4. The wave amplitude at first increases exponentially, reaches the value $\frac{1}{2}B$ at time $\tau = 0$ and then oscillates about its final value B as $\tau \to \infty$. The

https://doi.org/10.1017/S0022112002001246 Published online by Cambridge University Press

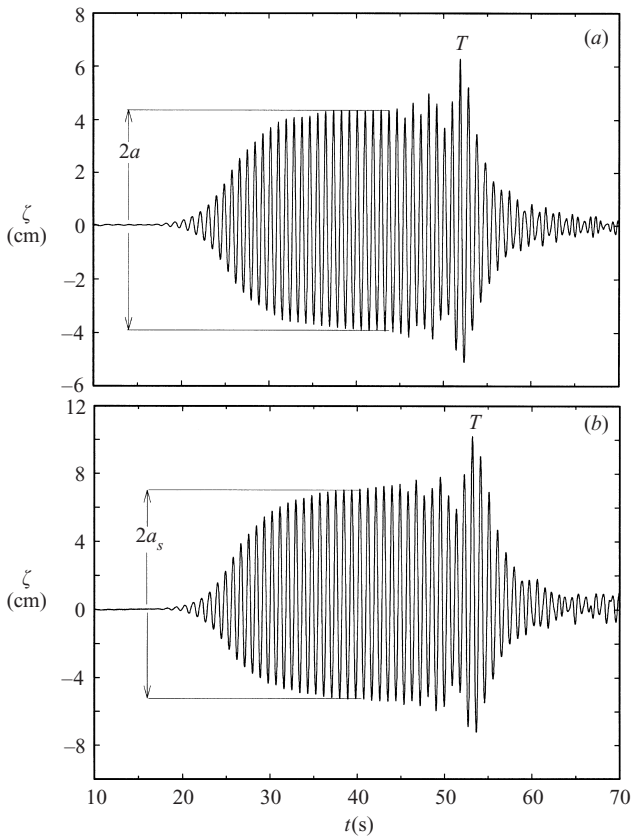


FIGURE 6. Surface elevation at $x = 15.65$ m when $G = 1.6$ (a) with no barrier and (b) with the barrier in place.

first maximum in the amplitude is about 19% greater than the final amplitude. It has been shown experimentally (see Longuet-Higgins 1976) that the effect of finite wave steepness is to increase the effective group velocity so that the wave front arrives slightly sooner than predicted by the linear theory, and to increase the maximum wave amplitude considerably.

In the present experiments, in order to suppress the oscillations of the envelope, the wavemaker was started gradually from rest with a horizontal displacement given by

$$\zeta = \begin{cases} 0, & t < 0 \\ C \tanh \lambda t \sin 2\pi f t, & t > 0, \end{cases} \tag{4.4}$$

where C and λ are constants. It was found convenient to take $\lambda = 0.1$. When λ was much smaller, the wave train often did not approach its final amplitude ($e^{-2\lambda t}$ negligible) before the onset of the three-dimensional instabilities mentioned above.

On the other hand, it was found useful to terminate the wave train after a certain number N of wave cycles, by switching off the wavemaker suddenly. This produced a corresponding Fresnel pattern of the wave envelope at the *rear* of the wave train, including some waves which were steeper than the steady waves.

The input voltage to the wavemaker was governed by a certain gain factor, which we have denoted by G. Experiments were carried out over the range $1.6 \leqslant G \leqslant 2.6$; see table 1 for the corresponding wave parameters.

https://doi.org/10.1017/S0022112002001246 Published online by Cambridge University Press

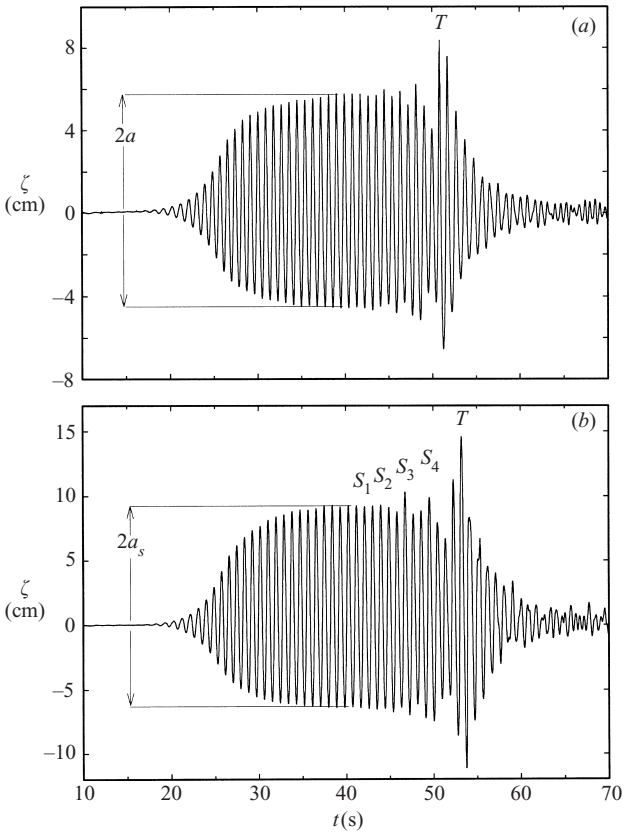


FIGURE 7. Surface elevation at $x = 15.65$ m when $G = 2.0$ (*a*) with no barrier (*b*) with the barrier in place.

At each value of the gain G, four types of measurements were made. First, the surface elevation ζ was recorded at a point close to the wavemaker ($x = 2.30$ m) but still far enough away that local effects were negligible, in general. The barrier at B was not in place. Second, similar measurements were made at the point B, still without the barrier, so that the waves passed by as progressive waves. Thirdly the barrier was inserted, and the surface elevation was recorded at the same point B. In all three cases the wave gauge was situated on the centreline of the channel. Simultaneously with the third recording, a video sequence of the waves near the barrier was taken as described above.

In order to prevent any horizontal displacement of the barrier it was constructed of 1.0 in. laminated plywood, strengthened by angle brackets, and was secured in place by a steel bar at the top, clamps above the water level and a firm tubular rubber seal at each sidewall. During the experiment no surface waves on the down-wave side of the barrier were detected.

A step-calibration of the wire wave gauges was carried out at the beginning and end of each series of experiments.

5. Results

Figures 5 and 6 show the case $G = 1.6$. In figure 5 we see the wave amplitude at $x = 2.30$ m starting almost immediately to increase monotonically towards the value

https://doi.org/10.1017/S0022112002001246 Published online by Cambridge University Press

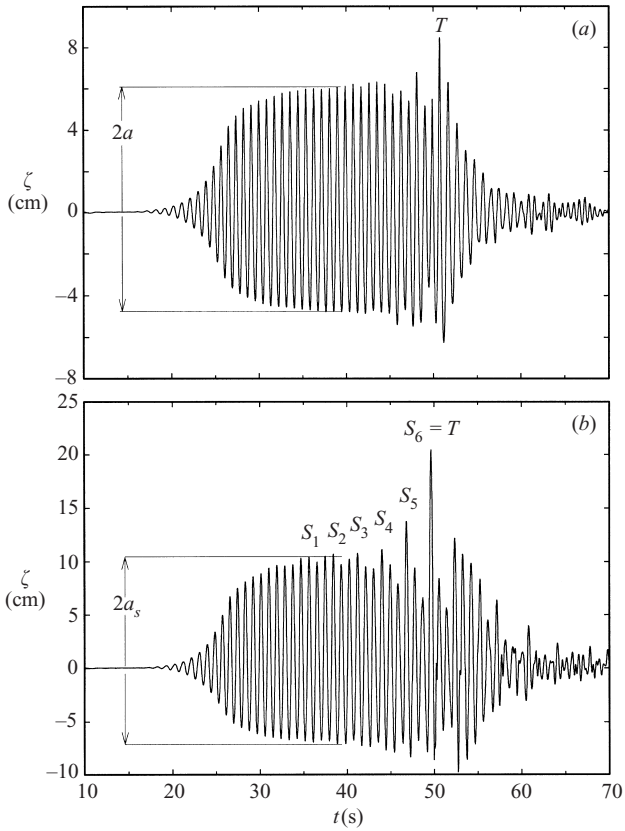


FIGURE 8. Surface elevation at $x = 15.65$ m when $G = 2.2$ (a) with no barrier (b) with the barrier in place.

4.5 cm, which is attained after about 25 s. At $t = 38$ s one can see the maximum T of the Fresnel envelope created by the abrupt shut-off of the wavemaker after 40 cycles (36 s).

Figure 6(a) shows the same progressive wave train on arriving at B ($x = 15.65$ m). The final amplitude a is now only 4.2 cm, attained at about $t = 35$ s. It remains constant until about $t = 42$ s, after which it is affected by the Fresnel pattern from the wave cut-off. From equation (4.2) the width of the Fresnel pattern is proportional to $(2x/g)^{1/2}$ and so is increased over the width at $x = 2.30$ m by a factor 2.61. When $t > 30$ s there are slight indications of a Benjamin–Feir instability, but these are small compared to the oscillations of the Fresnel envelope. The period of the envelope oscillations diminishes with distance from T. When $t = 43$ s their period is less than two wave periods.

Figure 6(b) shows the same situation as 6(a) but with the barrier in place. Note the difference in vertical scales. The wave amplitude a_s is roughly equal to $2a$ (see table 1) as one would expect from linear theory.

The corresponding three records when $G = 1.8$ were quite similar to those in figures 5 and 6, but with larger amplitudes; see table 1. However when $G = 2.0$ some qualitatively new features appeared. Figures 7(a) and 7(b) show the records taken at the point B ($x = 15.65$ m) without the barrier and with the barrier in place, respectively. Figure 7(a) shows the usual Fresnel envelope for a progressive wave, with

https://doi.org/10.1017/S0022112002001246 Published online by Cambridge University Press

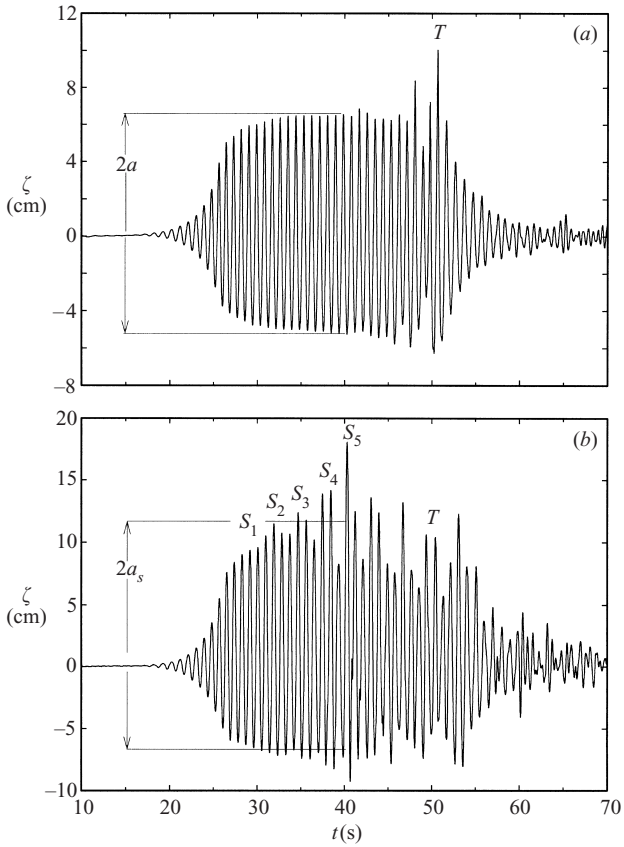


FIGURE 9. Surface elevation at $x = 15.65$ m when $G = 2.4$ (a) with no barrier (b) with the barrier in place.

the maximum at T. Before $t = 40$ s there is a slight modulation of the envelope due either to a Benjamin–Feir instability or to some three-dimensionality in the motion. Figure 7(b), however, taken with the barrier in place, shows that between $t = 40$ s and $t = 50$ s there is apparently a new instability in which every third wave, marked with the symbol S_i ($i = 1$ to 4) is higher than its two neighbours.

This is confirmed by figures 8(a) and 8(b), taken when $G = 2.2$. In figure 8(b), which shows the surface elevation in the reflected wave, the three-fold pattern now extends as far as from $t = 35$ s to $t = 50$ s. It appears to have overwhelmed the Fresnel pattern even as far as the maximum T.

Figure 9(b), corresponding to $G = 2.4$, shows the same pattern extending as far back as $t = 30$ s, but by $t = 45$ s the waves have become chaotic and the Fresnel pattern is quite ragged. A similar phenomenon is apparent in figure 10(b), corresponding to $G = 2.6$. Here the pattern begins and breaks down even earlier.

An examination of the photographic record, see figure 11 for the case $G = 2.4$, reveals that the highest peaks in each triplet are always sharp-pointed. The lower peaks are either round-crested or flat-topped or sometimes have profiles that are of intermediate form; see figure 11. After the crest S_5, at $t = 40$ s, the motion becomes markedly three-dimensional, which contributes to the chaotic appearance of the record of surface elevation.

https://doi.org/10.1017/S0022112002001246 Published online by Cambridge University Press

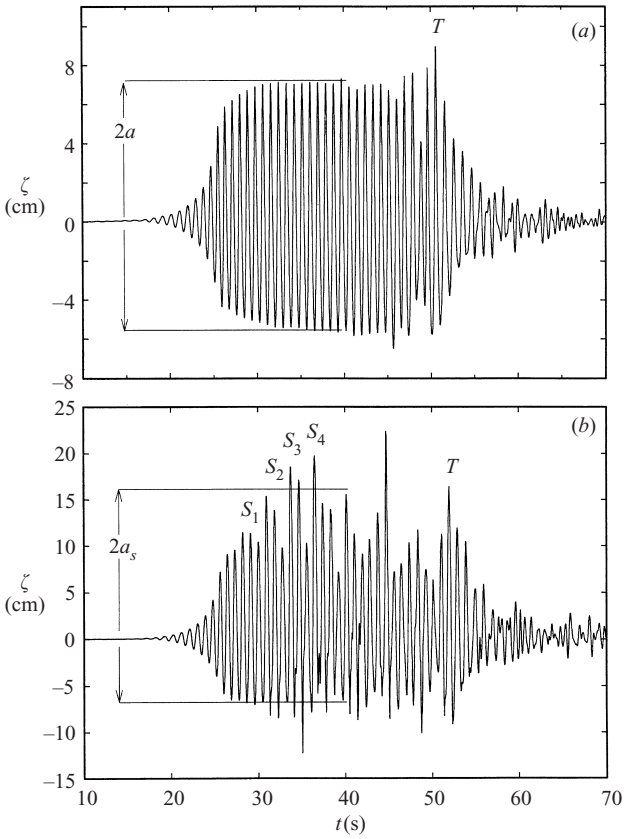


FIGURE 10. Surface elevation at $x = 15.65$ m when $G = 2.6$ (a) with no barrier (b) with the barrier in place.

6. Discussion and conclusions

A rough measure of the amplitude of the instability noted in figures 7(b) to 10(b) is the difference $\Delta\zeta$ in crest height between the highest and lowest waves of each triplet. In figure 12, $\Delta\zeta$ has been plotted against the suffix i in S_i on a log-linear scale, for each value of G, except that when $G = 2.6$, i has been increased by 2 to bring the plots closer together. (This does not of course affect the proportional rate of increase of $\Delta\zeta$.) It will be seen that in every case except one, namely $i = 1$ and $G = 2.0$, the plots lie close to the same straight line. This indicates an increase in $\Delta\zeta$ by a factor of about 2.2 for every three wave cycles, that is an increase of 1.3 per wave cycle. The exceptional plotted point (shown in parentheses) corresponds to a very small value of $\Delta\zeta$, lying within the noise-level of the experiment.

Thus we have detected a subharmonic instability which tends to occur at values of G greater than about 2.0, that is to say incident wave steepnesses $ak \geqslant 0.236$ (see table 1). The observed rate of growth is about 1.3 per wave cycle, practically independent of the incident wave amplitude.

The above instability is probably related dynamically to the 'period tripling' phenomenon observed by Jiang *et al.* (1998) in forced standing waves. There are some differences, however.

(1) In Jiang *et al.* (1998) standing waves were forced subharmonically by oscillating the wave tank vertically at a frequency twice that of the resulting surface waves. Such

https://doi.org/10.1017/S0022112002001246 Published online by Cambridge University Press

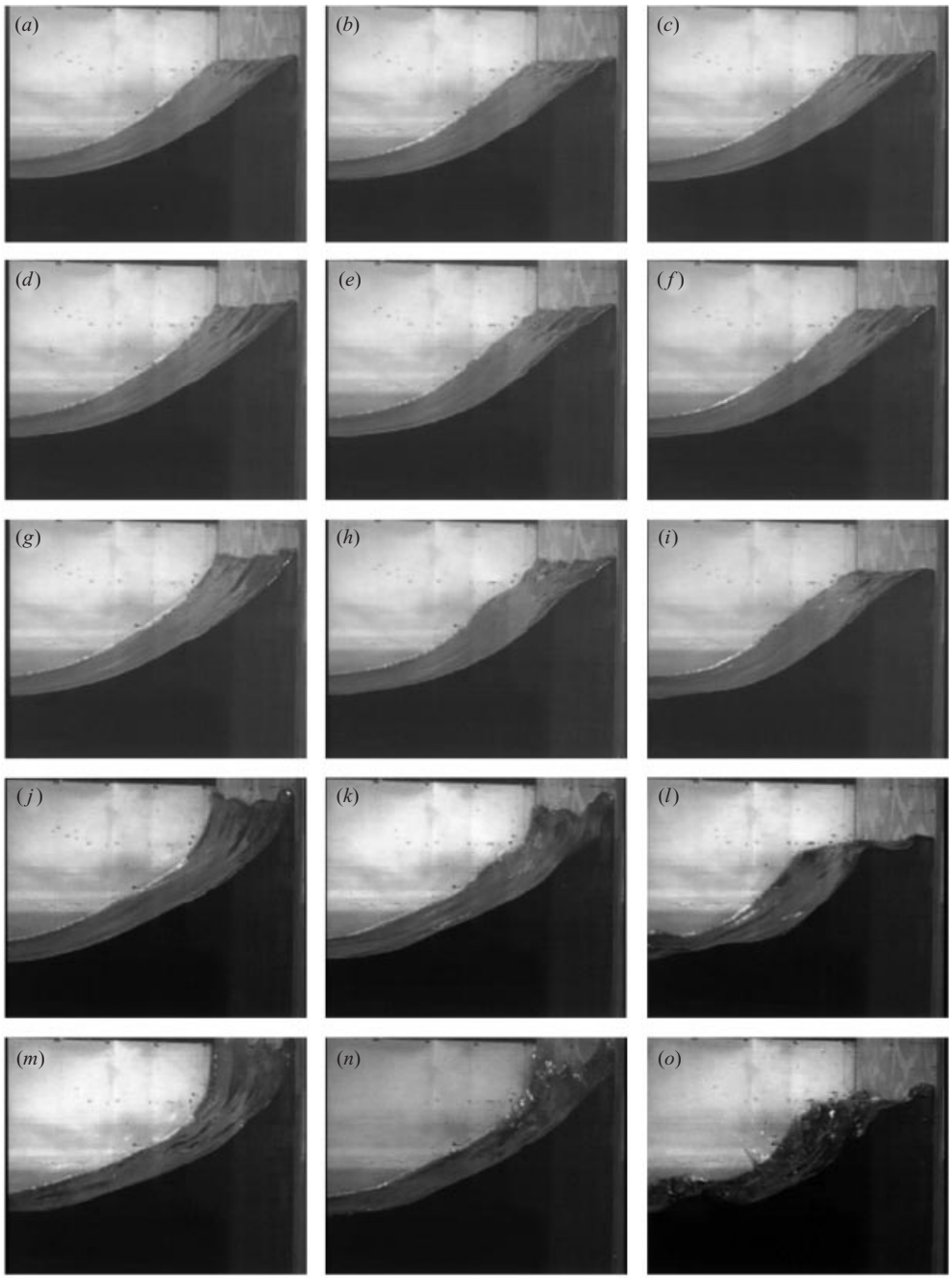


FIGURE 11. A sequence of frames from the video corresponding to figure 9(*b*) ($G = 2.4$), showing consecutive wave crests between $t = 28$ s and 42 s. The video was taken at 30 frames/s, and the timing of each frame is as close as possible to a maximum of the surface elevation shown in figure 9(*b*), that is within 1/60 s. Each frame in the left-hand column above corresponds to one of the maxima marked S_i in figure 9(*b*).

https://doi.org/10.1017/S0022112002001246 Published online by Cambridge University Press

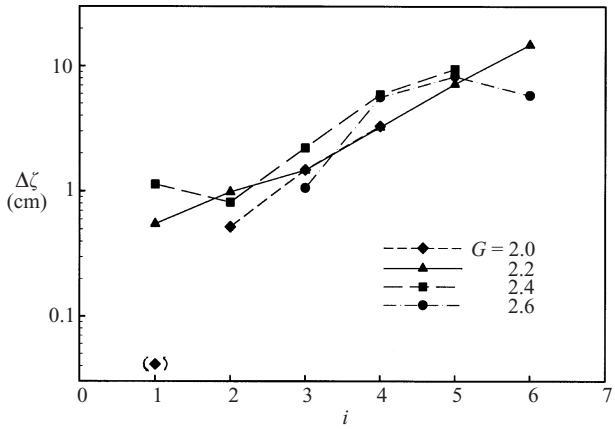


FIGURE 12. Growth of the triple-period instability, as measured by the difference $\Delta\zeta$ in crest-elevation between the highest and lowest waves of a triplet.

a method of excitation is of course unlikely to be found in nature except, for example, in an earthquake at sea. In our experiments the 'quasi-standing' waves were the result of the reflection of free progressive waves from a vertical cliff or wall.

(2) In the experiments of Jiang *et al.* (1998) a *steady* state was achieved by balancing the input of wave energy from the vertical forcing against the loss of energy due to wave breaking. In our experiments there was no energy input due to vertical motion of the bottom, the loss of energy due to wave breaking was negligible, and the instability grew in time.

(3) In their experiments the observed sequence of wave crests was: sharp-crested → flat-topped → rounded → sharp-crested, and so on. In our experiments a sharp-crested wave was often *preceded* by a flat-topped wave, though not invariably. Other types of crest form were also observed, as illustrated in figure 11.

Note that some instabilities of periodic standing waves that are subharmonic in space were found analytically by Mercer & Roberts (1992). Those described here, however, were subharmonic in time. Recording of the spacial behaviour of the instability as a function of the horizontal coordinate x would have involved much more elaborate instrumentation, particularly since the position of the wave crests, other than at the wall, appeared to be slightly variable.

In the profiles shown in figure 11 the effects of both viscosity and surface tension are apparently negligible. Viscous effects at the vertical barrier would tend to be reduced by the oscillatory nature of the boundary layer. Although surface tension may affect the wave profiles at smaller scales, at larger scales one can expect Froude scaling to apply.

M.S.L.H. is supported by the Office of Naval Research under Contract N00014-00-1-0248, and D.A.D. by the National Science Foundation under Grant OCE-98-12182 to W. K. Melville. The authors thank C. Coughran, J. Lyons and D. Aglietti for technical assistance. An account of the experiments was presented at the INI Program on Surface Water Waves, Cambridge, England, 13–31 August 2001, and at the IMA Conference on Wind-over-Waves, Churchill College, Cambridge, 3–5 September 2001.

https://doi.org/10.1017/S0022112002001246 Published online by Cambridge University Press

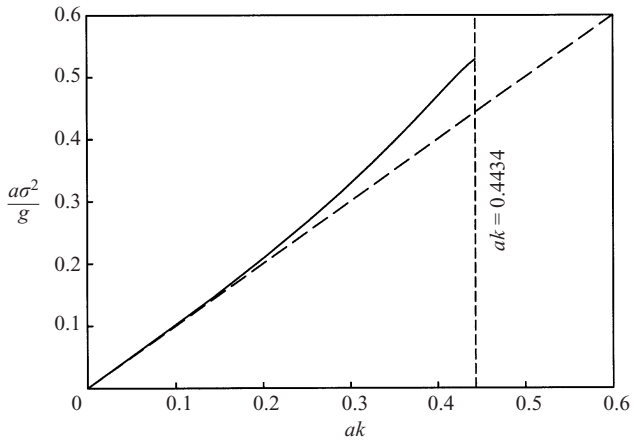


FIGURE 13. Graph of $a\sigma^2/g$ against ak for nonlinear progressive gravity waves in deep water.

ω	ak	(c^2-1)	$a\sigma^2/g$
0.00	0.00000	0.00000	0.00000
0.10	0.14222	0.02042	0.14512
0.20	0.20216	0.04173	0.21060
0.30	0.24877	0.06385	0.26465
0.40	0.28843	0.08674	0.31349
0.50	0.32346	0.11020	0.35911
0.55	0.33958	0.12203	0.38102
0.60	0.35488	0.13384	0.40238
0.65	0.36936	0.14552	0.42311
0.70	0.38303	0.15687	0.44312
0.75	0.39582	0.16767	0.46219
0.80	0.40765	0.17757	0.48000
0.85	0.41839	0.18601	0.49621
0.90	0.42782	0.19211	0.51001
0.95	0.43578	0.19454	0.52056
10.00	0.4432	0.1931	0.5288

TABLE 2. Corresponding values of ak and $a\sigma^2/g$ for deep-water gravity waves of finite amplitude.

Appendix. Determination of the steepness parameter *ak*

Given the crest-to-trough wave height $2a$ and the radian frequency $\sigma = 2\pi/T$, where T is the wave period, our problem is to find the wave steepness ak, where k is the wavenumber.

It is assumed that the waves are effectively in deep water, that is to say if h is the still-water depth, then e^{-2kh} is negligible. Now in table 2 of Longuet-Higgins (1975), the phase-speed c and the quantity

$$a/\pi = 2a/L = 2ak \tag{A 1}$$

are both given as functions of a monotonic parameter ω which runs from 0 to 1 as the wave passes from zero steepness to its limiting configuration with a sharp-angled crest. See also figure 1 of that paper, where ak and (c^2-1) are both plotted against ω. From the tabulated entries we may thus obtain the first three columns of table 2

https://doi.org/10.1017/S0022112002001246 Published online by Cambridge University Press

below. Hence for each value of ak we find the corresponding value of

$$a\sigma^2/g = (c^2/g)\,ak. \tag{A 2}$$

The values are plotted in figure 13. In the experiments, σ^2/g is a known constant. Hence for every value of a we can calculate $a\sigma^2/g$ and by interpolation in figure 13 find the corresponding value of ak.

REFERENCES

Abramowitz, M. & Stegun, I. A. 1964 *Handbook of Mathematical Functions*. Washington, D.C., US Govt. Printing Office, 1046 pp.

Chan, E. S. & Melville, W. K. 1988 Deep-water plunging wave pressures on a vertical wall. *Proc. R. Soc. Lond.* A **417**, 95–131.

Jiang, L., Perlin, M. & Schultz, W. W. 1998 Period tripling and energy dissipation of breaking standing waves. *J. Fluid Mech.* **369**, 273–299.

Longuet-Higgins, M. S. 1975 Integral properties of periodic waves of finite amplitude. *Proc. R. Soc. Lond.* A **342**, 157–174.

Longuet-Higgins, M. S. 1976 Breaking waves – in deep or shallow water. In *Proc. 10th Symp. on Naval Hydrodynamics*, Cambridge, Mass., June 1974 (ed. R. D. Cooper & S. W. Doroff), pp. 597–605. Arlington, VA, Office of Naval Research, 792 pp.

Longuet-Higgins, M. S. & Dommermuth, D. G. 2001*a* On the breaking of standing waves by falling jets. *Phys. Fluids* **13**, 1652–1659.

Longuet-Higgins, M. S. & Dommermuth, D. G. 2001*b* Vertical jets from standing waves. II. *Proc. R. Soc. Lond.* A **457**, 2137–2149.

Mercer, G. N. & Roberts, A. J. 1992 Standing waves in deep water: their stability and extreme form. *Phys. Fluids* A **4**, 259–269.

Miles, J. W. 1962 Transient gravity wave response to an oscillating pressure. *J. Fluid Mech.* **13**, 145–150.

https://doi.org/10.1017/S0022112002001246 Published online by Cambridge University Press